Assessing terrain shifts and infrastructure impact: a dual approach using satellite imagery and UAV data in the Cibedug, Rongga landslide

Moch Hilmi Zaenal Putra[1*], *Adrin* Tohari[1], *Achmad* Fakrus Shomim[1], *Eko* Soebowo[1], *Yayat* Sudrajat[1], *Amar*[1], *Wahyudin*[1], and *Dwi* Sarah[1]

[1]Geological Disaster Research Center, National Research and Innovation Agency, Bandung, Indonesia

Abstract. This study investigates the Rongga landslide, located on the southwest-facing slope of the southern mountain range in West Java, Indonesia, which is particularly prone to landslides due to its geological composition and topographical features. The research integrates high-resolution satellite imagery and UAV data to analyse the vertical, horizontal, and rotational displacements caused by the landslide. Vertical displacement was observed at the main crown, right flank, and left flank, with variations ranging from 1.5 to 4 meters. Horizontal movement was quantified across different zones of the landslide, with the upper zone experiencing the greatest displacement of 6.5 meters, and the lower zone showing the least at 3 meters. Rotational movements were significant in the upper and lower zones but were absent in the middle zone. This comprehensive analysis provides valuable insights into the dynamics of the Rongga landslide and lays the groundwork for future mitigation strategies.

1 Introduction

Landslides on volcanic deposits in mountainous regions provide significant hazards especially to surrounding settlements and infrastructure [1]. Volcanic deposits, composed of loose materials such as ash, pyroclastic rocks, and lahar, indicate low stability, particularly when influenced by intense and prolonged rainfall or seismic activity [2]. This instability can cause the material to move rapidly down slopes, resulting in large-scale landslides, leading to extensive landslides that could wipe out houses, roadways, and agricultural land along their track [3]. Moreover, the unconsolidated characteristics of volcanic deposits promote erosion, further exacerbating landslide risks. The impacts of such landslides surpass mere material destruction, potentially resulting in fatalities, disruption of transportation networks, and extensive environmental effects, including river erosion and flash floods in downstream regions [4]. Consequently, research and mitigation efforts are essential for minimising the hazards of landslides in volcanic areas and mitigating their impacts on local residents and ecosystems [5].

The analysis of land movement prior to and following landslides is essential for comprehending the dynamics of terrain shifts and their effects on infrastructure. Recent research has emphasised the efficacy of integrating satellite imagery and UAV data to monitor and analyse geohazards, with a particular emphasis on the displacement of structures as a critical indicator. The utilisation of high-resolution satellite images to identify precursors to landslides was demonstrated by Casagli et al. (2017), which enabled the early detection of potential dangers to structures [6]. Similarly, Niethammer et al. (2012) demonstrated the accuracy of unmanned aerial vehicles (UAVs) in the capture of detailed post-event terrain changes, which provided essential data on the displacement of structures and other infrastructure [7]. These studies emphasise the significance of utilising pre- and post-landslide imagery to accurately evaluate land movement and its effects on structures, thereby improving our capacity to anticipate future landslides and devise effective mitigation strategies. The comprehensive approach to detecting and analysing the displacement of buildings in landslide-prone areas is provided by the combination of detailed, high-resolution data from UAVs and a wide coverage of satellite images.

The combination of these datasets is highly effective for a comprehensive analysis of land movement. Pre-landslide satellite imagery provides extensive coverage that is appropriate for detecting large-scale land movements and trends that preceded the event, whereas post-landslide UAV imagery offers precise, high-resolution, and detailed measurements of the affected area [8]. The study's accuracy and depth are enhanced by the immediate, high-detail response provided by UAV imagery and the historical comparison facilitated by satellite imagery. This integrated approach enhances the accuracy of models that predict future landslides and assists in the development of effective mitigation strategies by combining the precise, timely data from

* Corresponding author: mochhilmizp@gmail.com

UAVs with the broad coverage and historical context of satellite images [9, 10].

2 Study area

The Rongga landslide (Fig. 1), which is located on the southwest-facing slope of the southern mountain range in West Java, was the primary focus of the investigation. In the lower section of the landslide, it is situated adjacent to the sinuous Bank River of Cidadap, a river that is approximately 30 kilometres in length and originates from Mount Tambaga Ruyung/Tambak Ruyung. The river passes through eight villages in West Bandung Regency (KBB): Mekarwangi, Gununghalu, Sirnajaya, Bunijaya, Sindangjaya, Cicadas, Cibedug, and Bojong. These villages are situated in three districts: Sindangkerta, Gununghalu, and Rongga. The landslide has an average slope of 12° and covers elevations ranging from 1020 meters at the crown to 980 meters at the toe. The landslide is primarily located in the Tmc formation, which is composed of interbedded claystone, siltstone, and sandstone, as well as localised lahar deposits of tuff, andesite breccia, and tuff breccia [11]. The Tmc formation's geological characteristics, structural complexities, and mountainous topography put this region particularly susceptible to landslides.

3 Methodology

3.1 Data collection

This study utilizes two primary sources of data to assess land movement and building displacement before and after landslide events: high-resolution satellite imagery from Google Earth Pro and UAV (Unmanned Aerial Vehicle) data. The integration of these datasets allows for a comprehensive analysis of terrain shifts and their impact on infrastructure, particularly focusing on the displacement of buildings and infrastructures.

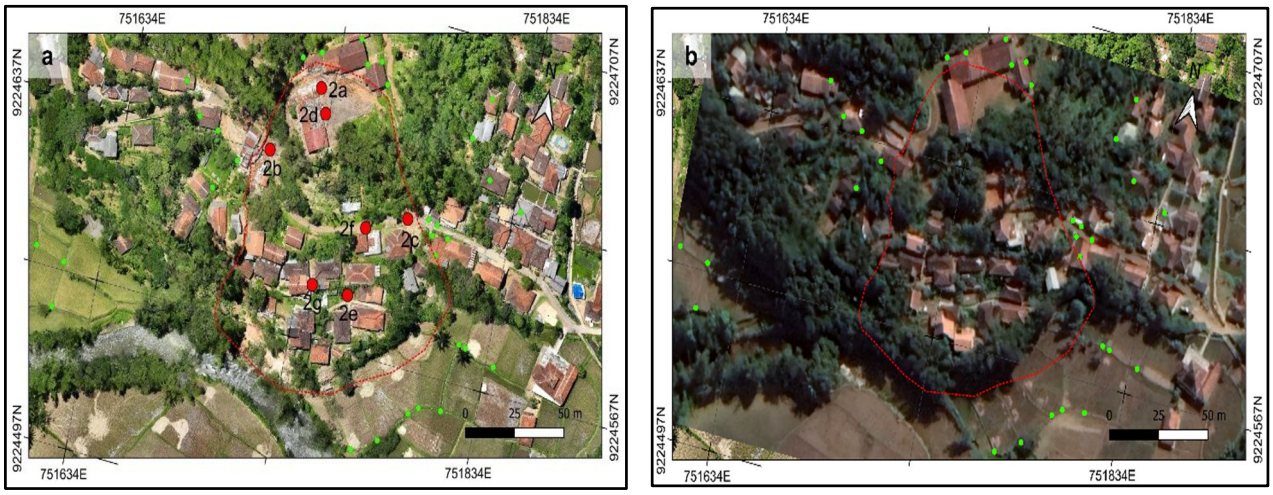

(a) (b)

Fig. 1. Pre-processing stage. Two images (a. after, b. before) are aligned using ground control point (GCP) data (green points) based on identifiable and stable features such as buildings and landscape elements unaffected by the landslide.

3.1.1 Pre-landslide data: google earth pro

Pre-landslide data was acquired from Maxar Technologies via Google Earth Pro in June 2018. The satellite imagery provided through this platform offers a resolution ranging from 0.3 to 0.5 meters per pixel, which is sufficient for identifying broad patterns of land movement over large areas. The high-resolution images also serve as a historical baseline for comparing changes over time. The multispectral capabilities of this imagery enable analysis across different spectral bands, which is useful for identifying vegetation stress and soil types. The georeferencing of these images ensures precise mapping and alignment with other datasets, facilitating accurate spatial analysis.

3.1.2 Post-landslide data: UAV imagery

Post-landslide data was collected using the DJI Matrice 350 RTK (M350) UAV. This UAV is capable of achieving ground sampling distances as fine as 1-2 centimeters per pixel, offering a high level of detail necessary for assessing small-scale displacements. The RTK technology and the D-RTK 2 GNSS mobile station provide centimeter-level accuracy in positioning, ensuring precise measurements of building movements. The UAV captured high-resolution images from various angles and altitudes, providing detailed and customizable coverage of the affected area. Additionally, the UAV's multispectral imaging capabilities allow for detailed post-event vegetation and soil analysis. Rapid deployment of the UAV enabled timely data collection immediately after the landslide event, ensuring that the most critical changes were documented. This post-landslide data was collected on March 20 2024, 16 days after the landslide incident on March 4 2024 as can be seen in Table 1.

Table 1. The detail of data

	Pre-Landslide Data	**Post-Landslide Data**
Type	Google Earth Pro Historical Imaginary	UAV Imagery
Tools / Source	Maxar Technologies via Google Earth Pro	DJI Matrice 350
Date Acquisition	June, 2018	March 20, 2024
Resolution	0.3 – 0.5 m	1 - 2 cm

3.2 Data processing and analysis

3.2.1 Pre-processing

The pre-landslide satellite images and post-landslide UAV images were georeferenced to a common coordinate system to ensure accurate spatial comparison. This involved aligning the images based on known ground control points (GCPs).

Distinctive features in stationary regions, such rooftop corners, road crossings, and rice field boundaries, were utilised as ground control points (GCPs) between the pre- and post-landslide images. The fixed points serve as dependable reference sites that facilitate the precise alignment of the two image sets. The light green points represent the dispersion of the specified Ground Control Points (GCPs) for this georeferencing operation. The distribution of these GCPs throughout the research region markedly improved the spatial accuracy of the comparison between the satellite and UAV images. This method facilitated accurate identification of changes in the landscape, encompassing the magnitude and shift induced by the landslide.

3.2.2 Displacement analysis

The displacement analysis involved a two-step process to detect and quantify changes in building positions due to landslides. Firstly, change detection was performed using image differencing techniques. By comparing pre- and post-landslide images, changes in the terrain were identified, with particular focus on areas where buildings had significantly shifted. This technique allowed for the detection of even subtle displacements, providing an initial indication of affected structures.

Secondly, a quantitative assessment was conducted to measure the exact displacement of buildings. This involved identifying key structural points on buildings in both the pre- and post-landslide images and calculating the shifts in their positions. Horizontal displacement was measured to determine the extent of movement. By combining these methods, the analysis provided a comprehensive understanding of how buildings were impacted by the landslide, highlighting areas of concern and aiding in the development of mitigation strategies.

3.2.3 Integration and validation

The findings from the satellite and UAV data were integrated to provide a comprehensive view of the land movement. The satellite images offered broad coverage and historical context, while the UAV data provided detailed, high-resolution measurements. The integration of these datasets enabled a more accurate assessment of building displacement.

To validate the results, field surveys were conducted where possible to compare the measured displacements with on-ground observations. This validation step ensured the reliability and accuracy of the remote sensing data and the derived measurements.

By leveraging the strengths of both satellite and UAV imagery, this methodology provides a robust framework for assessing the displacement of buildings and other infrastructure following a landslide, enhancing our understanding of the dynamics of such geohazards, and aiding in the development of effective mitigation strategies.

4 Result and discussion

4.1 Vertical displacement

The landslide caused significant ground subsidence across various sections of the affected area. As shown in Fig. 2a, the main crown subsided by approximately 4 meters. The right flank, depicted in Fig. 2b, experienced a drop of 3.5 meters, while the left flank, shown in Fig. 2c, subsided by 2 meters. Fig. 2a was taken on May 22, 2024, whereas Fig. 2b and 2c were captured 10 days after the incident, on March 14, 2024. The locations where these photos were taken are indicated in Fig. 1a.

4.2 Horizontal displacement

In addition to vertical movement, the landslide also experienced horizontal displacement. We will divide the discussion of this horizontal movement into three sections: upper, middle, and lower. In the upper section, around Babakan Talang 01 Elementary School, field observations indicated visible horizontal displacement. However, this movement could not be quantified because the area became a crushing zone, obscuring markers that could indicate the extent of horizontal displacement. Based on displacement analysis between pre- and post-event imagery, a horizontal movement toward the south of approximately 6.5 meters was observed (Fig. 3). This measurement was derived from the displacement of unique features, specifically the edge of the roof of Babakan Talang 01 Elementary School and the side of the road on the right flank of the landslide.

In the lower section, around the blue house that experienced rotation, severe damage was evident, with visible signs of movement. Displacement analysis between pre- and post-event imagery indicated a horizontal shift to the south by approximately 5 meters. This displacement differed significantly from the previous measurement, with a difference of 1.5 meters. However,

close to the river bank in the lower section, the displacement increased again to 5 meters.

In the middle zone, encompassing the road and residential areas, damage was minimal. Unlike the upper zone (around Babakan Talang 01 Elementary School) and the lower zone (the tilted blue house), the middle area showed only minor cracks on house walls, and the ground appeared largely unaffected, with no visible cracks. Field observations suggested no significant movement in this middle zone. However, displacement analysis between pre- and post-event imagery revealed a horizontal shift to the south of approximately 5 meters. This displacement was 1 meter less than in the upper zone but 2 meters greater than in the lower zone.

Overall, vertical displacement is evident from the outcrops observed, such as at the main crown, the right flank, and the left flank of the landslide, with vertical changes ranging from 1.5 to 4 meters. Horizontal displacement can be quantified through image analysis before and after the landslide. All sections of the landslide, including the upper, middle, and lower zones, experienced horizontal movement, with variations ranging from 3 to 6.5 meters. The greatest horizontal displacement occurred in the upper zone, at the Babakan Talang 01 Elementary School building, while the smallest was observed in the lower zone, at the blue house, particularly at its scarp, which underwent significant rotation. Rotational movement was absent in the middle zone, whereas rotation was clearly observed at the main scarp in the upper zone and the minor scarp in the lower zone. The collection of data on horizontal, vertical, and rotational movements, with varying displacements in each section, will help in understanding the characteristics of the Rongga landslide and support further analysis.

Fig. 2. The locations where these photos (a-g) were taken are indicated in Fig. 1a. **a.** The main crown forms a clear horseshoe-shaped scarp, with a significant elevation difference of up to 4 meters. Dark and light brown soil material is exposed along the scarp. **b.** The outcrop on the right flank of the landslide, which severed access to the main road and destroyed nearby buildings, shows a subsidence of 3.5 meters. **c.** The outcrop on the left side of the landslide, which also cut off access to the main road, shows a subsidence of 1.5 meters. **d.** The change in elevation at SDN Babakan Talang 01, where buildings within the landslide zone experienced a subsidence from their original level. **e.** The lower zone showing significant rotation of up to 30 degrees, supported by evidence such as tilted utility poles, footpaths, and buildings. **f.** The middle zone, which shows no signs of rotational movement, with minimal landslide features, such as the absence of cracks in buildings and main roads, and trees remaining upright. **g.** The difference in rotational forces between the middle and lower zones, where buildings and trees in the middle zone remain upright, while in the lower zone they are tilted.

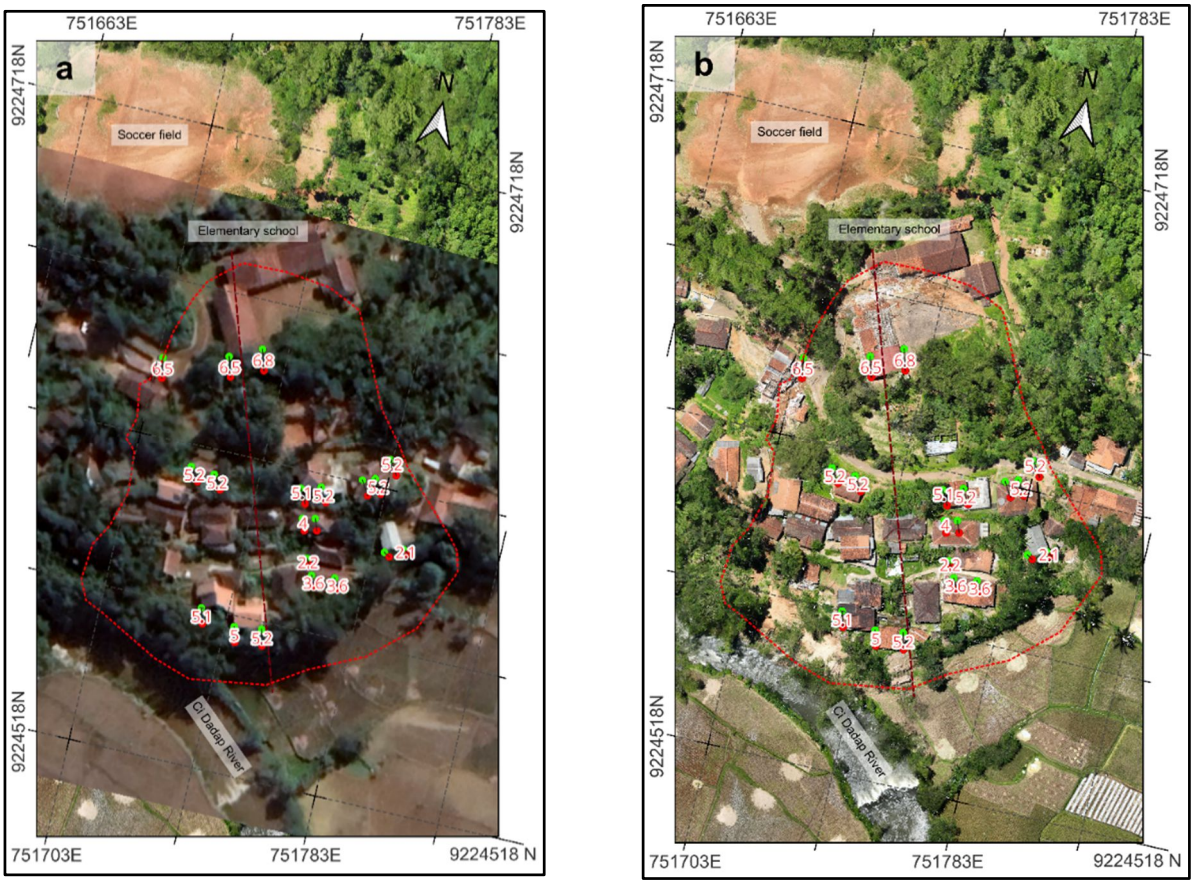

Fig. 3.: Map showing the overall movement of buildings and roads affected by the landslide. green and red points indicate the positions a) before and b) after. The landslide event occurred on march 4, 2024.

5 Conclusions

The Rongga landslide presented a multifaceted pattern of displacement, marked by significant vertical, horizontal, and rotational movements across various zones. Vertical displacement ranged from 1.5 to 4 meters, with the most pronounced changes occurring at the main crown, which highlights the differential movement within the landslide area. The horizontal displacement was also notable, with the upper zone experiencing the largest shift of 6.5 meters, while the lower zone exhibited a smaller movement of 3 meters. The absence of rotational movement in the middle zone, compared to the distinct rotational shifts in both the upper and lower zones, underscores the varying impact of the landslide across different sections. These findings emphasize the complex nature of the landslide and the need for a tailored approach to mitigation efforts in similar geological settings.

One of the strengths of this study lies in the integration of high-resolution satellite imagery and UAV data, which provided a comprehensive view of the landslide's dynamics. The combination of these two data sources allowed for a detailed analysis of both large-scale trends and small-scale changes, offering a more nuanced understanding of the landslide's impact on the terrain and infrastructure. However, the study also had some limitations. The precision of displacement measurements, particularly in the upper and lower zones, was affected by the resolution of the satellite imagery and the potential for UAV data distortion due to environmental conditions during data capture. Additionally, while the study provided valuable insights into the immediate aftermath of the landslide, it did not account for potential long-term changes in the landscape, which could be crucial for ongoing monitoring and mitigation efforts.

To build upon the results of this study, future research could benefit significantly from integrating these findings with geotechnical and geophysical analyses. Incorporating geotechnical studies, such as soil sampling and laboratory analysis, would provide a deeper understanding of the material properties that contributed to the landslide's behaviour. Geophysical methods, such as seismic refraction or electrical resistivity tomography (ERT), could complement the UAV and satellite data by offering subsurface insights that are not visible in surface imagery alone. Additionally, integrating these results with advanced numerical modelling and simulation could help predict the future behaviour of the landslide under various environmental conditions, such as intense rainfall or seismic activity.

The combination of geological, geophysical, and laboratory analyses with advanced modelling techniques would offer a more comprehensive understanding of the landslide mechanisms at play. By creating models that integrate both surface and subsurface data, researchers could develop more accurate predictions and risk assessments for future landslides in similar regions. This

multi-disciplinary approach would not only deepen the understanding of landslide dynamics but also inform the design of more effective mitigation strategies, potentially reducing the impact of such events on vulnerable communities and infrastructure.

Future studies should also address the limitations identified in this research by incorporating longer-term monitoring to capture the evolution of the landslide over time. This could involve repeated UAV surveys at different intervals to observe ongoing changes in displacement and refine the accuracy of horizontal and vertical movement measurements. Additionally, integrating other remote sensing technologies, such as LiDAR or InSAR, could enhance data precision, particularly in areas where UAV or satellite imagery might be less effective due to environmental factors. Expanding the study to include a broader range of environmental and geological factors, such as rainfall patterns and seismic activity, could further enhance the understanding of landslide triggers and progression. Such approaches would not only improve predictive models for future landslides but also contribute to the developments of more robust and effective mitigation strategies.

This research is funded by Rumah Program Kebencanaan Hidrometeorologi dan Iklim - Organisasi Riset Kebumian dan Maritim - Badan Riset dan Inovasi Nasional (BRIN), Indonesia for 2024. The authors would like to thank for supporting them for conducting this work.

References

1. M. H. Z. Putra, R. D. Kartiko, P. Soemantidiredja, I. A. Sadisun, and A. Tohari, Pengaruh Zona Jenuh Air Terhadap Kestabilan Lereng Di Weninggalih, Kabupaten Bandung Barat, Ris. Geol. dan Pertamb., **30**(1), 119, 2020.
2. F. Fusco et al., Physically Based Estimation of Rainfall Thresholds Triggering Shallow Landslides in Volcanic Slopes of Southern Italy, Water, **11(**9), (2019).
3. K. Mertens et al., The direct impact of landslides on household income in tropical regions: A case study from the Rwenzori Mountains in Uganda, Sci. Total Environ., **550**, 1032–1043, (2016).
4. A. K. Turner, Social and environmental impacts of landslides, Innov. Infrastruct. Solut., **3(**1), 1–25, (2018).
5. X. Fan et al., Earthquake-Induced Chains of Geologic Hazards: Patterns, Mechanisms, and Impacts, Rev. Geophys., **57**(2), 421–503, (2019).
6. N. Casagli et al., Landslide mapping and monitoring by using radar and optical remote sensing: Examples from the EC-FP7 project SAFER, Remote Sens. Appl. Soc. Environ., **4**, 92–108, (2016).
7. U. Niethammer, M. R. James, S. Rothmund, J. Travelletti, and M. Joswig, UAV-based remote sensing of the Super-Sauze landslide: Evaluation and results, Eng. Geol., **128**, 2–11, (2012).
8. S. Chen, C. Xiang, Q. Kang, W. Zhong, Y. Zhou, and K. Liu, Accurate landslide detection leveraging UAVbased aerial remote sensing, IET Commun., **14**(15), 2434–2441, (2020).
9. I. Farmakis, E. Karantanellis, D. J. Hutchinson, N. Vlachopoulos, and V. Marinos, Superpixel and Supervoxel Segmentation Assessment of Landslides Using UAV-Derived Models, Remote Sens., **14(**22), (2022).
10. K. Yang, W. Li, X. Yang, and L. Zhang, Improving Landslide Recognition on UAV Data through Transfer Learning, Appl. Sci., **12**(19), (2022).
11. M. Koesmono, Kusnama, and N. Suwarna, Geological Map of The Sindangbarang and Bandarwaru Quadrangles, Jawa. 2nd Edition. Geological Research and Development Centre, 1996.